ELSEVIER

Remote Sensing of Environment 81 (2002) 416–426

Remote Sensing of Environment

www.elsevier.com/locate/rse

Integrated narrow-band vegetation indices for prediction of crop chlorophyll content for application to precision agriculture

Driss Haboudane[a,*], John R. Miller[a,b], Nicolas Tremblay[c], Pablo J. Zarco-Tejada[d], Louise Dextraze[c]

[a]Centre for Research in Earth and Space Science (CRESS), York University, Petrie Science Building, 4700 Keele Street, Toronto, ON, Canada M3J 1P3
[b]Department of Physics and Astronomy, York University, Toronto, ON, Canada M3J 1P3
[c]Agriculture and Agri-Food Canada Research Branch, Horticulture Research and Development Centre, 430 Boulevard Gouin, St-Jean-sur-Richelieu, QC, CanadaJ3B 3E6
[d]Department of Land, Air, and Water Resources (LAWR), Center for Spatial Technologies and Remote Sensing (CSTARS), University of California-Davis, Davis, CA 95616-8671, USA

Received 25 April 2001; received in revised form 15 January 2002; accepted 19 January 2002

Abstract

Recent studies have demonstrated the usefulness of optical indices from hyperspectral remote sensing in the assessment of vegetation biophysical variables both in forestry and agriculture. Those indices are, however, the combined response to variations of several vegetation and environmental properties, such as Leaf Area Index (LAI), leaf chlorophyll content, canopy shadows, and background soil reflectance. Of particular significance to precision agriculture is chlorophyll content, an indicator of photosynthesis activity, which is related to the nitrogen concentration in green vegetation and serves as a measure of the crop response to nitrogen application. This paper presents a combined modeling and indices-based approach to predicting the crop chlorophyll content from remote sensing data while minimizing LAI (vegetation parameter) influence and underlying soil (background) effects. This combined method has been developed first using simulated data and followed by evaluation in terms of quantitative predictive capability using real hyperspectral airborne data. Simulations consisted of leaf and canopy reflectance modeling with PROSPECT and SAILH radiative transfer models. In this modeling study, we developed an index that integrates advantages of indices minimizing soil background effects and indices that are sensitive to chlorophyll concentration. Simulated data have shown that the proposed index Transformed Chlorophyll Absorption in Reflectance Index/Optimized Soil-Adjusted Vegetation Index (TCARI/OSAVI) is both very sensitive to chlorophyll content variations and very resistant to the variations of LAI and solar zenith angle. It was therefore possible to generate a predictive equation to estimate leaf chlorophyll content from the combined optical index derived from above-canopy reflectance. This relationship was evaluated by application to hyperspectral CASI imagery collected over corn crops in three experimental farms from Ontario and Quebec, Canada. The results presented here are from the L'Acadie, Quebec, Agriculture and Agri-Food Canada research site. Images of predicted leaf chlorophyll content were generated. Evaluation showed chlorophyll variability over crop plots with various levels of nitrogen, and revealed an excellent agreement with ground truth, with a correlation of $r^2 = .81$ between estimated and field measured chlorophyll content data. © 2002 Elsevier Science Inc. All rights reserved.

1. Introduction

Remote sensing data and techniques have already proven to be relevant to many requirements of crop inventory and monitoring. Different studies and experiments demonstrated their usefulness and feasibility to address various agricultural issues, such as crop classification and mapping (Erol & Akdeniz, 1996; Grignetti, Salvatori, Cascchia, & Manes, 1997; Pax-Lenney & Woodcock, 1997), crop forecasting and yield predictions (Clevers, 1997; Moran, Maas, & Pinter, 1995; Rasmussen, 1992; Tucker, Holben, Elgin, & McMurtrey, 1980), crop status and condition (Blackmer, Schepers, & Varvel, 1994; Boissard, Pointel, & Huet, 1993; Clevers, Büker, van Leeuwen, & Bouman, 1994; Potdar, 1993), and crop disease and micronutrient deficiency (Adams, Norvell, Philpot, & Peverly, 2000a, 2000b; Adams, Philpot, & Norvell, 1999; Malthus & Madeira, 1993). Nowadays, there is an increased interest in precision farming and the development of smart systems for agricultural resources management; these relatively new approaches aim

* Corresponding author. Fax: +1-416-736-5626.
E-mail address: driss@terra.phys.yorku.ca (D. Haboudane).

0034-4257/02/$ – see front matter
PII: S0034-4257(02)00018-4

to increase the productivity, optimize the profitability, and protect the environment. In this context, image-based remote sensing technology is seen as a key tool to provide valuable information that is still lacking or inappropriate to the achievement of sustainable and efficient agricultural practices (Daughtry, Walthall, Kim, Brown de Colstoun, & McMurtrey, 2000; Moran, Inoue, & Barnes, 1997). More specifically, farmers and agricultural managers are interested in measuring and assessing soil and crop status at specific critical times: first, in earlier growth stages in order to supply adequate fertilizers quantities for a normal growth of the crop, and second, during an advanced development stage for health monitoring and the prediction of yield. For this purpose, remote sensors can play a valuable role in providing time-specific and time-critical information for precision farming, due to their capabilities in measuring biophysical indicators/parameters and detecting their spatial variability. The latter is critical to the variable rate technology, which consists of applying specific inputs, such as fertilizers, for specific soil and crop conditions (Moran et al., 1997). Among the fertilizing elements, nitrogen is generally the most important and also the major limiting factor for crop growth and agriculture productivity.

Nitrogen concentration in green vegetation is related to chlorophyll content, and therefore indirectly to one of the basic plant physiological processes: photosynthesis. When nitrogen supply surpasses vegetation's nutritional needs, the excess is eliminated by runoff and water infiltration leading to pollution of aquatic ecosystems (i.e., eutrophication) (Wood, Reeves, & Himelrick, 1993, cited in Daughtry et al., 2000). This nitrogen loss to the environment represents an economic loss for farmers. However, inappropriate reduction of nitrogen supply could result in reduced yields, and subsequently, substantial economic losses. With this dilemma, the optimal and rational solution is an adequate assessment of nitrogen status and its variability in agricultural landscapes. Since yield is determined by crop condition at the earlier stages of growth, it is mandatory to provide farmers with nitrogen status at those stages in order to supply appropriate rates based upon an accurate assessment of plant growth requirements and deficiencies.

For this purpose, remote sensing techniques have been used to assess crop conditions relative to nitrogen status and effects. Foliage spectral properties, reflectance and transmittance, were found to be affected by nitrogen deficiency (Blackmer, Schepers, Varvel, & Walter-Shea, 1996): nitrogen shortage reduces leaf chlorophyll content, and therefore, increases its transmittance at visible wavelengths. Thus, reflected radiation from crop leaves and canopies has been used both to estimate chlorophyll concentration of crop canopies (Daughtry et al., 2000) and by implication to assess nitrogen variability and stress (Blackmer et al., 1994, 1996). However, at the canopy scale, nitrogen treatments do not affect leaf chlorophyll content alone; they also induce differences in other biophysical parameters such as: Leaf Area Index (LAI), biomass, and foliage (Walburg, Bauer, Daughtry, & Housley, 1982). Moreover, optical indices developed for chlorophyll content estimation, using crop canopy reflected radiation, are responsive to other vegetation and environmental parameters like LAI and underlying soil reflectance (Daughtry et al., 2000; Kim, Daughtry, Chappelle, McMurtrey, & Walthall, 1994).

It is this multifactor interaction complexity, responsible for canopy spectral reflectance variability at different phenological stages, that inspired this work on developing a methodology for an accurate estimation of crop chlorophyll content. The objectives were: (i) to simulate corn canopy reflectance, using PROSPECT and SAILH radiative transfer models, for various crop optical and biophysical variables; (ii) to elaborate a methodology for estimating crop chlorophyll concentration, using CASI hyperspectral airborne reflectance data; and (iii) to validate the estimates through a comparison with chlorophyll measurements in the laboratory from plot field sampling.

2. Material and methods

2.1. Study area

The study area is one of the four experimental sites of the GEOmatics for Informed Decisions (GEOIDE) project for precision agriculture. It is located near Montreal, at the Horticultural Research and Development Centre of Agriculture and Agri-Food Canada, St-Jean-sur-Richelieu, Quebec, Canada, also known as the L'Acadie experimental research substation, where corn was grown on four adjacent experimental fields. In general, the soils in the fields were clay loam, with 31% sand, 33% silt, and 36% clay in the 0–30-cm layer. The median pH_w was 6.8 and the average phosphorus and potassium levels measured were, respectively, 72 and 147 mg/kg of dry soil. Both these values are characterized as rich by the Conseil des productions végétales du Québec. The fields had various cropping histories, and the actual $N-NO_3$ concentration at seeding time varied from one field to the next (52, 27, 51, and 37 kg $N-NO_3$/ha in the 0–60-cm layer for fields 40, 41, 48, and 49, respectively; see Fig. 9). In each field, there were four experimental blocks, each containing four 20×20-m plots, to which the nitrogen fertilizer treatments were randomly assigned. Each plot was made up of 27 rows of planted corn. In each field, a weedy plot and a bare soil plot were set up between the two pairs of blocks. Nitrogen fertilization treatments were supplied in two applications: one at the time of seeding, the other at top dressing 6 weeks later. The experiment comprised a total of 64 experimental plots representing a wide range of nitrogen levels. Four major treatments have been supplied: (A) no fertilization, (B) intermediate fertilization with uniform nitrogen application at top dressing and (C) with variable nitrogen application at top dressing based on early chlorophyll content measurements, and (D) overfertilization, representing a reference plot saturated in chlorophyll. For further details on nitrogen treatments, quantities, and application procedures, the reader is referred to the paper by Tremblay, Miller, Haboudane, Bélec, and Dextraze (2001).

2.2. Airborne and field data

Hyperspectral images were acquired by the Compact Airborne Spectrographic Imager (CASI), flown by Centre for Research in Earth and Space Technology (CRESTech), as part of intensive field campaigns organized by the GEOIDE *Precision Agriculture* (RES54) project coinvestigators during Summer 2000. At the same time, various field and laboratory data were collected for biochemical and geochemical analysis, optical and biophysical measurements, along with other types of sensors' measurements (Fluorescence, Hydro N-Sensor). Other relevant ground truth measurements include: (i) collection of leaf tissue for laboratory determination of leaf chlorophyll concentration, (ii) corn leaf reflectance and transmittance measurements using an integrating sphere (Li-Cor model 1800-12) coupled by a single mode fibre to a spectrometer (Ocean Optics model ST-1000), (iii) chlorophyll meter (Minolta SPAD 502) measurements, (iv) LAI measurements using the Plant Canopy Analyzer (Li-Cor model LAI-2000), and (v) crop growth measures. The most recently expanded leaves of four plants per experimental unit were brought to the laboratory where one leaf disk (10 mm^2 each) was cut from each leaf to be used in the analysis of chlorophyll-*a* and -*b* content. The disks were stored at -20 °C until the chlorophyll analysis could be carried out. They were ground and the chlorophyll pigments were extracted in two successive portions of cold methanol (-20 °C). The material was completely colorless by the end of this process. The two portions were mixed and the concentration was measured according to Porra, Thompson, and Kriedemann (1989).

CASI hyperspectral images were collected in three different deployments, using two modes of operation: the *multispectral mode*, with 1-m spatial resolution and seven spectral bands suitable for sensing vegetation properties (489.5, 555.0, 624.6, 681.4, 706.1, 742.3, and 776.7 nm) and the *hyperspectral mode*, with 2-m spatial resolution and 72 channels covering the visible and near-infrared portions of the solar spectrum from 408 to 947 nm with a bandwidth of 7.5 nm. Acquisition dates were planned to coincide with different phenological development stages, but were disturbed by the bad weather prevailing during that summer. Nevertheless, three missions were successfully performed, providing image data covering the earliest, middle, and latest periods of the growth season.

2.3. CASI hyperspectral data processing

The processing of CASI imagery included the following separate stages: raw data to radiance transformation, atmospheric corrections and reflectance retrieval, removal of aircraft motion effects and georeferencing, and flat field adjustments of surface reflectance spectra.

The hyperspectral digital images collected by CASI were processed to at-sensor radiance using calibration coefficients determined in the laboratory by CRESTech. Then the CAM5S atmospheric correction model (O'Neill et al., 1997) was used to transform the relative at-sensor radiance to absolute ground reflectance. To perform this operation, an estimate of aerosol optical depth at 550 nm was derived from ground sun photometer measurements and Aerosol Robotic NETwork (AERONET, 2000) website. Reflectance spectra of asphalt and concrete within CASI imagery were used to calculate coefficients that adequately compensate for residual effects of atmospheric water and oxygen absorption, and therefore to perform the flat field calibration. Data regarding geographic position, illumination, and viewing geometry as well as ground and sensor altitudes were derived both from aircraft navigation data recordings and ground GPS measurements.

2.4. Simulated leaf reflectance and transmittance

Leaf optical properties were simulated using the PROSPECT model (Jacquemoud & Baret, 1990; Jacquemoud et al., 1996), which simulates upward and downward hemispherical radiation fluxes between 400 and 2400 nm, and relates foliar biochemistry and scattering parameters to leaf reflectance and transmittance spectra. It requires the leaf internal structure parameter N, the chlorophyll-*a* and -*b* content C_{ab} (μg/cm^2), the equivalent water thickness C_w (cm), the leaf protein content C_p (g/cm^2), and leaf cellulose and lignin C_c (g/cm^2) to determine leaf reflectance and transmittance signatures in the optical domain.

Input parameters C_w, C_p, and C_c were assigned the nominal values of 0.001 cm, 0.0012 g/cm^2, and 0.002 g/ cm^2, respectively. The N parameter has been estimated by inverting the PROSPECT model on corn reflectance and transmittance spectra measured in the laboratory using an integrating sphere coupled to a spectrometer. The mean value 1.41 thereby obtained is in agreement with the value ($N=1.4$) used for corn plants by Jacquemoud, Bacour, Poilve, and Frangi (2000). With these inputs, reflectance and transmittance spectra were generated for chlorophyll content varying from 0 to 70 μg/cm^2 for two purposes: investigating the performance of the Modified Chlorophyll Absorption in Reflectance Index (MCARI) (Daughtry et al., 2000) and simulating corn canopy reflectance (SAILH model) for a wide range of chlorophyll concentrations.

2.5. Simulated canopy reflectance

Canopy reflectance spectra were simulated using a variant of the SAIL (Scattering by Arbitrary Inclined Leaves) model (Verhoef, 1984) called SAILH. It was adapted to take into account the hotspot effect or the multiple scattering in the canopy (Kuusk, 1985). It is a turbid-medium model that approximates the canopy as a horizontally uniform parallel-plane infinitely extended medium, with diffusely reflecting and transmitting elements. Discussions and mathematical formalisms of SAIL and SAILH are found in Goel (1988, 1989), Verhoef (1984, 1998), and Zarco-Tejada (2000). Typical SAILH inputs are: canopy architecture defined by the LAI and the leaf angle distribution function (LADF), leaf reflectance and transmittance spectra for given chlorophyll content per unit area, underlying soil reflectance, and the illumination and viewing geometry (solar zenith and sensor viewing angles).

Because the CASI instrument acquires hyperspectral data in the visible and near-infrared portions of the solar spectrum, simulations have been performed over the spectral range 400–825 nm, at a spectral increment of 5 nm. This is not a limiting factor as far as the central objective is chlorophyll content estimation. Indeed, chlorophyll interactions with the radiation are limited the optical domain ranging from 400 to 700 nm, while water and dry matter influences are observed beyond 900 nm (Jacquemoud et al., 2000). Thus, using a background soil reflectance extracted directly from the CASI imagery in bare soil plots, simulated spectra were calculated for 13 LAI values (0.1–8), 12 leaf chlorophyll contents (5–60 μg/cm^2), and three sun zenith angles (27°, 33°, and 45°) corresponding to those prevailing at the time of data acquisition (Table 1) in the three acquisition dates.

2.6. Spectral vegetation indices for chlorophyll estimation

Over recent years, expanding research activities have focused on understanding the relationships between vegetation optical properties and photosynthetic pigments concentrations within green leaves tissues, namely: chlorophyll-*a*, chlorophyll-*b*, and carotenoids. From the optical point of view, these pigments have different spectral behavior, with specific absorption features at different wavelengths, which allows remote sensing techniques to discriminate their respective effects on vegetation reflectance spectra (Blackburn, 1998a; Chappelle, Kim, & McMurtrey, 1992). These characteristics have promoted the development of various approaches, based on model inversion or the use of empirical and semiempirical methods, to estimate the chlorophyll content both at the leaf and canopy scales (Blackburn, 1998b; Datt, 1999; Daughtry et al., 2000; Demarez & Gastellu-Etchegorry, 2000; Gitelson, Merzyak, & Lichtenthaler, 1996; Zarco-Tejada, Miller, Noland, Mohammed, & Sampson, 2001). Among these investigations, studies using optical indices for chlorophyll estimation have focused on evaluating the reflectance in individual narrow bands, band reflectance ratios and combinations, and the characteristics of derivative spectra. They used different combinations of spectral bands to minimize variations owing to extraneous factors and maximize sensitivity to chlorophyll content. Their philosophy and formalism are based on the relationships existing between chlorophyll concentrations and some specific narrow spectral bands. The spectral regions that are identified as the most suitable to chlorophyll effects study are those around 680 nm, corresponding to absorption peak of chlorophyll-*a*, and 550 nm matching with the minimum chlorophyll absorption in the visible domain. Detailed discussions and thorough reviews concerning appropriate optimal wavelengths and chlorophyll indices can be found in publications such as those by Blackburn (1999) and Zarco-Tejada (2000). In the context of the present work, the focus is put on the index MCARI proposed by Daughtry et al. (2000) as a variant of the Chlorophyll Absorption in Reflectance Index (CARI) developed by Kim et al. (1994).

CARI was designed to reduce the variability of the photosynthetically active radiation due to the presence of diverse nonphotosynthetic materials. It uses bands corresponding to the minimum absorption of the photosynthetic pigments, centered at 550 and 700 nm, in conjunction with the chlorophyll-*a* maximum absorption band, around 670 nm. The choice of 700 nm is due to its location at the boundary between the region where vegetation reflectance is dominated by pigments absorption and the beginning of the red edge portion where vegetation structural characteristics have more influence on the reflectance (Kim et al., 1994). MCARI is a measure of the depth of chlorophyll absorption at 670 nm relative to the reflectance at 550 and 700 nm, and is quantified by the following equation where R_{ijk} is the reflectance at the *ijk*-th wavelength nanometer (Daughtry et al., 2000):

$$\mathrm{MCARI} = [(R_{700} - R_{670}) - 0.2(R_{700} - R_{550})](R_{700}/R_{670}). \tag{1}$$

Table 1
Input parameters for SAILH model

SAILH input parameters	Description/values
Leaf reflectance and transmittance	PROSPECT-simulated spectra for various chlorophyll content, from 5 to 60 μg/cm^2, in 5-μg/cm^2 steps
Soil reflectance	extracted from CASI imagery, clay loam soil, with 31% sand, 33% silt, and 36% clay in the 0–30-cm layer
LAI	0.1, 0.3, 0.5, 1, 1.5, 2, 2.5, 3, 4, 5, 6, 7, 8
Lead angle distribution function	spherical
Sun zenith angle	27°, 33°, and 45°
Sensor viewing angle	0° (nadir)
Fraction of direct coming radiation	1

The ratio (R_{700}/R_{670}) was introduced to minimize the combined effects of the underlying soil reflectance and the canopy nonphotosynthetic materials. This ratio is the slope of the spectrum when the canopy contains no green biomass. Nevertheless, MCARI is still sensitive to background reflectance properties so that it is difficult to interpret at low LAI (Daughtry et al., 2000).

Our interest in MCARI was motivated by its potential for use in an operational remote sensing scenario in the context of precision agriculture. Indeed, unlike derivative-based indices that are strongly correlated to chlorophyll concentration (Blackburn, 1999), MCARI does not require many contiguous narrow spectral bands. Even though MCARI was developed to be both responsive to chlorophyll variation and resistant to nonphotosynthetic materials effects, Daughtry et al. (2000) showed that MCARI is influenced by various parameters such as: LAI, chlorophyll, LAI–chlorophyll interaction, and the background reflectance. Moreover, our simulations have pointed out that MCARI is still sensitive to nonphotosynthetic element effects, mainly at low chlorophyll concentrations. To overcome these limitations, the present work suggests a modified MCARI version by improving its sensitivity at low chlorophyll values.

Kim et al. (1994) have shown that the change of background reflectance affects the reflectance slope between 550 and 700 nm. The ratio (R_{700}/R_{550}) differences are closely linked to the variations of reflectance characteristics of background materials (soil and nonphotosynthetic components). To compensate for these effects, the ratio (R_{700}/R_{670}) is used to counteract the background influence only on the difference ($R_{700} - R_{550}$) so that the Transformed Chlorophyll Absorption in Reflectance Index (TCARI) is defined as follows:

$$\mathrm{TCARI} = 3[(R_{700} - R_{670}) - 0.2(R_{700} - R_{550})(R_{700}/R_{670})]. \quad (2)$$

Despite the observed improvements regarding nongreen biomass effects, this intrinsic index is still sensitive to the underlying soil reflectance properties, particularly for low LAIs (Rondeaux, Steven, & Baret, 1996). In order to overcome this problem, Daughtry et al. (2000) proposed that MCARI be combined with a soil line vegetation index like Optimized Soil-Adjusted Vegetation Index (OSAVI; Rondeaux et al., 1996). Such an integration will reduce background reflectance contributions and enhance the sensitivity to leaf chlorophyll content variability. OSAVI belongs to the Soil-Adjusted Vegetation Index (SAVI; Huete, 1988) family and is defined by the following equation:

$$\mathrm{OSAVI} = (1 + 0.16)(R_{800} - R_{670})/(R_{800} + R_{670} + 0.16). \quad (3)$$

The reason that this index is selected, for this study, is due to its easy use in the context of operational observations on agricultural landscapes. In fact, its determination needs no information on soil optical properties, and moreover, it offered the best results for most agricultural crops (Rondeaux et al., 1996). Additionally, using CASI airborne data, we found that OSAVI has similar behavior and trends as Transformed Soil-Adjusted Vegetation Index (TSAVI; Baret, Guyot, & Major, 1989) whose determination requires the knowledge of soil line parameters. The latter should be calculated from image areas corresponding to bare soils. This assumes the presence of such areas in the observed scene, and depends on different soil conditions, like variations in moisture levels, to establish the soil line by plotting soil reflectance in red versus infrared space. These additional calculations (limitations) for TSAVI are not mandatory for OSAVI, thereby making the latter more suitable for observing and monitoring crops changes in the context of precision agriculture.

Unfortunately, the canopy reflectance shape results from a complex interaction between pigment concentrations, canopy structural development, and in some respects the underlying soil contribution. Moreover, vegetation indices that are insensitive to soil optical properties seem to be relatively insensitive to chlorophyll variations. Conversely, indices sensitive to chlorophyll content variability are strongly affected by the differences in the canopy LAI. For instance, Daughtry et al. (2000) found that LAI, chlorophyll, and chlorophyll–LAI interaction accounted, respectively, for 60%, 27%, and 13% of MCARI variation. Consequently, an accurate assessment of crop chlorophyll status from remotely sensed data requires spectral indices that are both responsive to chlorophyll concentration and insensitive to background and LAI effects. For this purpose, it has been demonstrated that a combined use of MCARI and OSAVI was successful in producing isolines of leaf chlorophyll concentrations (Daughtry et al., 2000). However, this combination was not implemented for predictive purposes nor have further developments dealt with LAI effects on pigment estimation from canopy reflectance measurements.

The present paper has introduced the use of the ratio TCARI/OSAVI to make accurate predictions of crop chlorophyll content from hyperspectral remote sensing imagery. The ratio has been shown to be relatively insensitive to canopy cover variations, even for very low LAI values. The determination of the leaf pigment predicting functions is based on simulations with PROSPECT and SAILH leaf and canopy models, and optical index scaling-up approach discussed in detail in Zarco-Tejada et al. (2001). Results of this approach are presented, discussed, and compared to ground truth measurements in the following section.

3. Results and discussion

3.1. Sensitivity to chlorophyll content

In a preliminary analysis for individual leaf spectra, chlorophyll indices MCARI (Eq. (1)) and TCARI (Eq. (2))

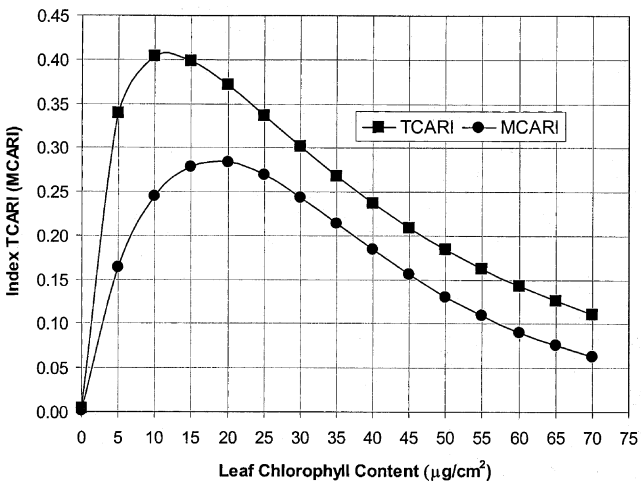

Fig. 1. Sensitivity to chlorophyll variability of TCARI and MCARI. Application to leaf-simulated reflectances using PROSPECT model.

were plotted as a function of chlorophyll content for leaf reflectances derived by simulations with the PROSPECT model (Fig. 1). As chlorophyll content increases, MCARI initially increases, but then decreases as chlorophyll content exceeds 20 μg/cm^2. This functional behavior denotes a sensitivity limitation of MCARI at low pigment concentrations, owing probably to its responsivity to nonphotosynthetic leaf material. Consequently, MCARI will be difficult to interpret because of the confounding effects induced by the trend inversion at 20 μg/cm^2: the same value of MCARI may correspond to two different pigment concentrations. The proposed TCARI exhibits a better sensitivity at low chlorophyll concentrations: it shows a negative correlation with chlorophyll content over a wider pigment range (10–70 μg/cm^2), but still a positive one for pigment content below 10 μg/cm^2 (Fig. 1). This is a useful improvement because leaf chlorophyll content is rarely less than 10 μg/cm^2. Nevertheless, as we intend to use TCARI for predictions at the canopy scale, there is a need to scale up these relationships to the canopy level through radiative transfer models and examine corresponding TCARI and MCARI canopy reflectance behavior. The next step is to evaluate these indices for above-canopy reflectance of an optically thick canopy, thereby assessing the effects of LAI and soil variations.

The optically thick vegetation medium reflectance (denoted here simply as infinite reflectance R_∞) can be approximately related to the single leaf reflectance r and transmittance t through the single leaf absorptance α ($\alpha = 1 - r - t$). Various infinite reflectance formulae could be found in literature (Zarco-Tejada, Miller, Mohammed, Noland, & Sampson, 2000); the one we used here (in Eq. (4)) characterizes the optically thick canopy with the single leaf absorption and scattering properties and assumes isotropic scattering (Hapke, 1993).

$$R_\infty = \frac{1 - \alpha^{1/2}}{1 + \alpha^{1/2}} \tag{4}$$

Fig. 2 highlights differences between MCARI and TCARI in terms of characterizing chlorophyll variations from remotely sensed data. While MCARI still shows weakness in predicting low chlorophyll concentrations, TCARI remains sensitive to chlorophyll variations over a wide range of concentrations including the lower one. However, both TCARI and MCARI drop to zero when chlorophyll content is 0 μg/cm^2. This means that bare soils will mimic high chlorophyll content values when TCARI (or MCARI) is used to predict chlorophyll variability from airborne or satellite remote sensing data. This point will be discussed later in the section concerning CASI hyperspectral data and ground truth. This drastic drop of TCARI over soil areas could be used as an advantage in the sense that TCARI could be used not only for mapping chlorophyll but also to map bare soils.

Now, at this intermediate scale, between the leaf level and the field one, a unique relationship exists between TCARI and chlorophyll concentrations, with coefficients of determination (r^2) exceeding .99 for different fitting functions (logarithmic, exponential, etc.) and for chlorophyll content ranging from 5 to 70 μg/cm^2. This result suggests strong potential for use in operational predictions with real data, but still there remains the uncertainty regarding the effects of structural development of the crops. LAI as a measure of the structural changes will be used in the next section to examine whether TCARI could resist those effects.

3.2. Sensitivity to LAI changes

The effects of plant growth (LAI) and chlorophyll content on MCARI and TCARI are illustrated in Figs. 3 and 4, respectively. It can be seen that the scaling up to the canopy level did not improve the sensitivity of MCARI at low pigment concentrations. Ambiguity in MCARI still exists for chlorophyll contents around 10 μg/cm^2 for all

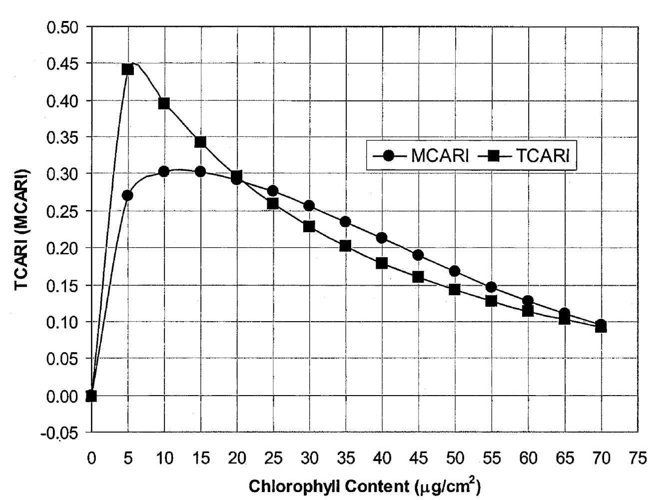

Fig. 2. Sensitivity to chlorophyll variability of TCARI and MCARI. Application to infinite reflectance determined for optically thick canopy.

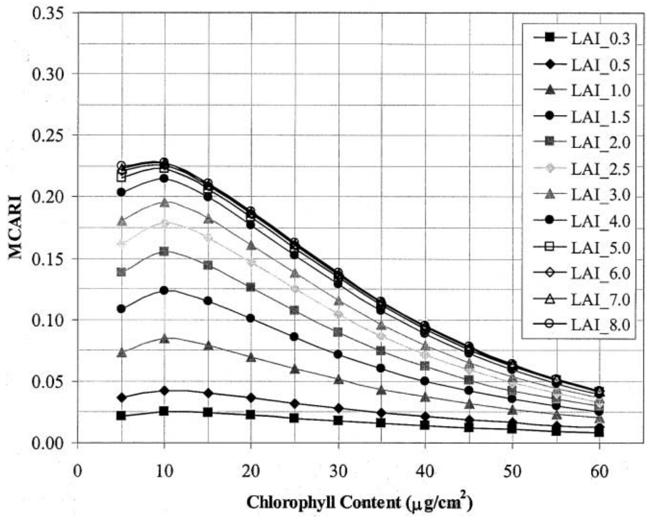

Fig. 3. Effects of LAI on MCARI sensitivity to chlorophyll content variation. Application to reflectance spectra simulated using PROSPECT and SAILH models.

LAI values (0.3–8) (Fig. 3). This phenomena is observed only at low foliage cover (LAI < 1) for TCARI, with smaller change rate (Fig. 4).

As expected, LAI exerts a strong influence on the relationships between both indices and the foliar pigments. It, however, contributes to more variability of MCARI than TCARI. The first shows high sensitivity to LAI changes at low and medium values (up to LAI = 2.5), while the second remains relatively less responsive to LAI variations even at low values (down to 1.5). In fact, for LAI values equal or greater than 1.5 and for the most observable chlorophyll concentrations (15–60 μg/cm^2), TCARI shows less variability and more resistance to the canopy structure change than MCARI does (Figs. 3 and 4). Moreover, the

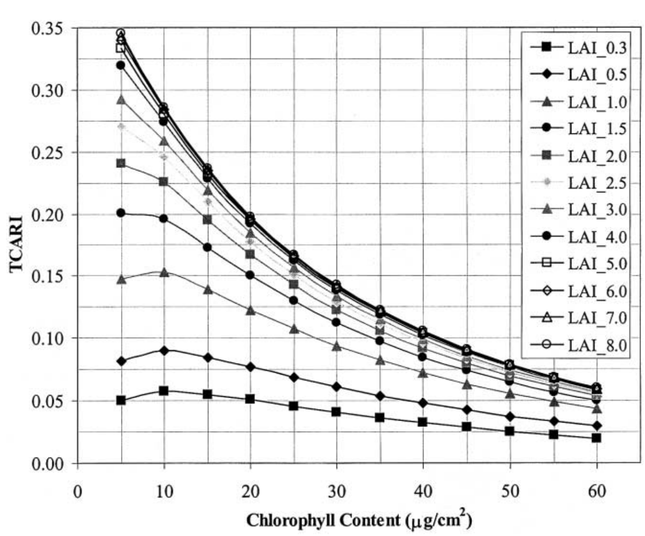

Fig. 4. Effects of LAI on TCARI sensitivity to chlorophyll content variation. Application to reflectance spectra simulated using PROSPECT and SAILH models.

average slope over the chlorophyll range 10–60 μg/cm^2 shows that TCARI is more sensitive to chlorophyll than MCARI. For instance, considering an LAI = 3, the average slopes are 0.41% and 0.32% for TCARI and MCARI, respectively. Consequently, given its lower responsivity to LAI variations and its sensitivity to chlorophyll changes, TCARI holds a consistent predictive ability for canopy chlorophyll estimation.

Despite these improvements, the problems related to low LAI values and LAI interaction with chlorophyll content remain unsolved. They are a source of uncertainty when it comes to make prediction in early vegetation growth stages. The latter corresponds to the most time-critical information needed by farmers and agricultural managers. During these early stages, soil reflectance dominates remotely sensed observations. Therefore, we combined TCARI with OSAVI in an attempt to uncouple the effects of LAI and leaf pigments. Fig. 5 shows the chlorophyll index TCARI plotted against the vegetation index OSAVI for various pigment contents and diverse foliage cover levels. Both indices are positively correlated with LAI: low TCARI and OSAVI values correspond to low LAI values and vice versa. Therefore, points representing bare soils will be concentrated near the scatter-plot origin (TCARI = 0, OSAVI = 0), while those corresponding to dense vegetation will be scattered in the opposite side around the major bisector.

The most important information revealed in Fig. 5 is the distribution of chlorophyll values in the OSAVI–TCARI space. For all foliage cover levels, chlorophyll concentrations are arranged along concentric arcs, with high values lying near the *x*-axis (OSAVI) and the low ones near the *y*-axis (TCARI). Moreover, points representing the same chlorophyll concentration, for different LAI values, are set along lines taking origins near the bare soil values. These chlorophyll isolines intersect near the scatter-plot origin and radiate outward as vegetation cover density increases. For clarity purposes, only the two isolines for low (5 μg/cm^2)

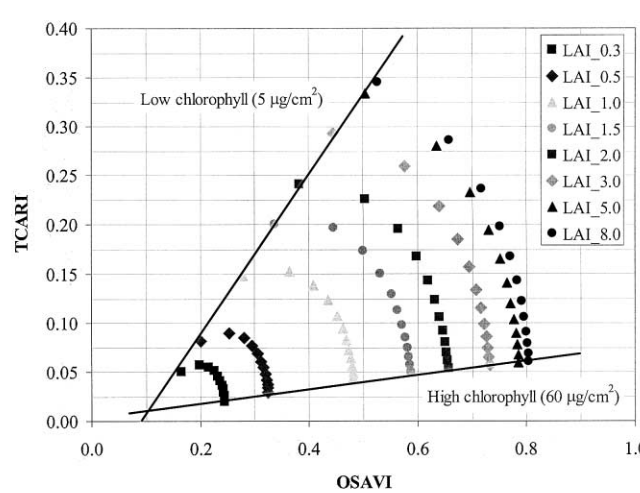

Fig. 5. Chlorophyll index TCARI plotted as a function of vegetation index OSAVI, for various chlorophyll concentrations and different LAI values.

and high (60 μg/cm^2) chlorophyll concentrations have been drawn. They show that slope of the isolines decreases with the increase of leaf chlorophyll content. Similar results have been reported by Daughtry et al. (2000) for three pigment concentration levels.

These findings suggest that chlorophyll content is correlated with the slope of TCARI versus OSAVI. Consequently, we determined the ratio TCARI/OSAVI and assessed its ability to take into account the effects of soil background reflectance and the crop structural development (LAI), aiming to derive a unique relationship between chlorophyll content and the combination TCARI/OSAVI. Indeed, and as expected, the ratio clearly combines the abilities of indices responding to chlorophyll variations and those minimizing background and LAI effects (Fig. 6). In comparison to MCARI and TCARI behavior (Figs. 3 and 4), the ratio drastically reduced the sensitivity to LAI effects while preserving a high sensitivity to chlorophyll variability. It exhibits a unique relationship with the chlorophyll content even over a wide range of LAI values (0.3–8). This is particularly consistent for the normal range of measured leaf chlorophyll content (15–60 μg/cm^2). With respect to extension of the predictions to low pigment contents (down to 5 μg/cm^2), a unique and consistent relationship could be determined for LAI values equal or greater than 0.5. These outcomes open the possibility to uncouple the linked contributions of chlorophyll and LAI to the canopy reflectance variation, and therefore, to accurately assess the chlorophyll status of crop canopies.

3.3. Chlorophyll predictions through TCARI/OSAVI

Through the analyses presented above, it is clear that the combined use of TCARI and OSAVI offers a great potential for estimating crop photosynthetic pigments. As shown in Fig. 7, predictive scaling-up relationships were established

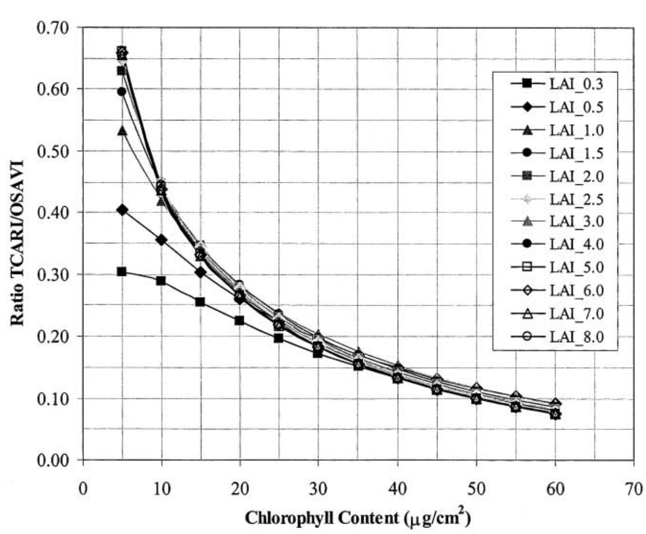

Fig. 6. Ratio TCARI/OSAVI plotted as a function of chlorophyll concentrations for various LAI values.

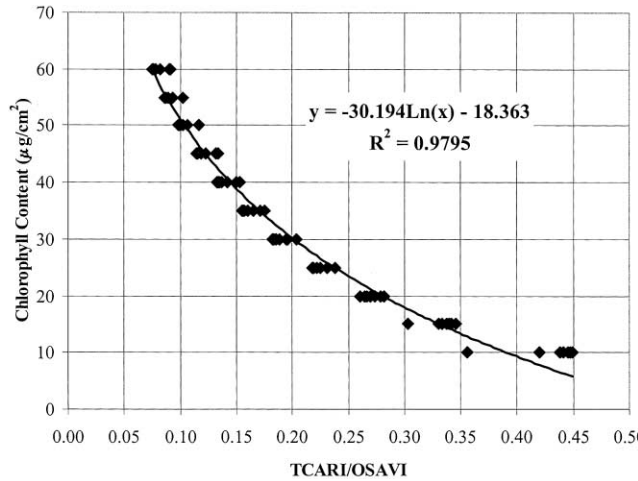

Fig. 7. Relationship between chlorophyll content and the ratio TCARI/OSAVI. Chlorophyll predictive function for LAI varying from 0.5 to 6 and chlorophyll concentrations ranging from 15 to 60 μg/cm^2.

to make chlorophyll estimations as a function of the ratio TCARI/OSAVI derived from above-canopy reflectance data. These relationships were determined for LAI values ranging from 0.5 to 6 and for chlorophyll concentrations varying from 10 to 60 μg/cm^2 (Fig. 7). For clarity purposes, LAI values exceeding six were not plotted because, as illustrated by Fig. 6, the ratio remains unchanged for LAI values greater than 3.

The best fits were obtained for logarithmic and polynomial functions, with determination coefficients (r^2) exceeding .98. Although polynomial functions fit the observed points better, the third order limits the prediction validity to the observed range. Consequently, logarithmic scaling-up relationships have been chosen as consistent estimates of chlorophyll concentrations. It is important to note that a slight dispersion of TCARI/OSAVI values occurs at low pigment concentrations, owing to the divergence induced by the low LAI value (0.5). However, this is not expected to affect the predictive ability since the predictive function coefficients (gain and offset) remain approximately the same (Fig. 7). Similar relationships have been found for different LAI ranges as well as for LAI different ranges. For brevity purposes and in order to prevent redundancy, they are not presented here.

It is of major importance to recall that these predictive functions were derived for soil reflectance and sun zenith angle typical of the observation condition (image of August 5, 2000) and for a spherical LADF. Considering that TCARI (MCARI) and OSAVI were developed to reduce optical effects of nonphotosynthetic materials and underlying soil, it is expected that the influence of the background reflectance has been taken into account; however, additional simulations would be required to confirm this assumption. Concerning solar zenith angle effects, as shown in Table 1, simulations have been conducted for three angles (27°, 33°, and 45°) corresponding to three dates of data collection.

Predictive equations were determined for these angles and found to be virtually identical. Indeed, their application for chlorophyll prediction leads to differences of less than 2.5%. Based on this, sun zenith angle seems to have negligible effect on estimation of chlorophyll status using TCARI/OSAVI. Regarding the LADF, further simulations are required to assess its influence on prediction functions.

3.4. Evaluation of chlorophyll predictions using airborne data

The ratio TCARI/OSAVI thus represents a spectral predictor of pigment concentrations at the canopy scale. Minimizing the perturbing effects of LAI variability, it shows a high correlation and a unique relationship with chlorophyll content. Using a logarithmic fit to the canopy simulation results described above, the ratio TCARI/OSAVI scaling-up tuned algorithm has been applied to CASI airborne hyperspectral images to map chlorophyll status over large areas of corn crops (L'Acadie experimental site). Results for the image of August 5, 2000, for which ground truth measurements are available, are reported here. The CASI bands chosen were 550.3, 671.0, 701.4, and 800.6 nm that were very close to recommended wavelengths for TCARI and OSAVI in Eqs. (2) and (3). Additional calculations (not shown here) using nearby wavelengths differing from the nominal by up to 5 nm revealed quick degradation of the LAI-insensitivity performance of the index.

Fig. 8 compares chlorophyll content estimations from CASI reflectance data and leaf chlorophyll content measurements in the laboratory from plot field sampling. It reveals a very good agreement between the predictions and the ground truth, with a coefficient of determination r^2=.804; the corresponding root mean square error (RMSE) is 4.35 μg/cm^2. In comparison with other recent studies that used the inversion of radiative transfer models for pigment content and LAI together over corn and soybean canopies, Jacquemoud et al. (2000) obtained determination coefficients (r^2) less than .58 (r < .77), although it should be noted that chlorophyll content was estimated with the SPAD meter, rather than directly measured from leaf samples. Therefore, the predictive capability of TCARI/OSAVI seems consistent and satisfactory.

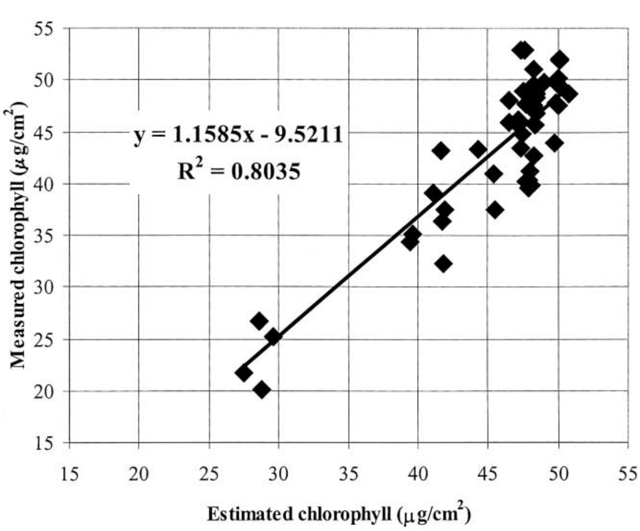

Fig. 8. Comparison between measured chlorophyll content and chlorophyll values estimated using the ratio TCARI/OSAVI. The RMSE is 4.35 μg/cm^2.

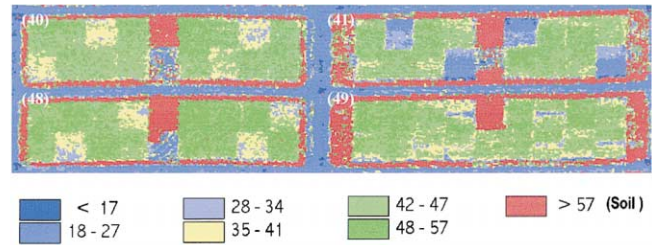

Fig. 9. Map of chlorophyll status determined from CASI hyperspectral image of August 5, 2000, for corn fields at the L'Acadie experimental site. Chlorophyll estimations have been performed through the relationship between chlorophyll concentration and ratio TCARI/OSAVI. Numbers 40, 41, 48, and 49 identify the fields described in the section Study Area. Chlorophyll content units are μg/cm^2.

The spatial distribution of chlorophyll status is illustrated by Fig. 9, where different plots have been discriminated according to their chlorophyll level. They correspond to various nitrogen treatments designed to study the link between nitrogen fertilization and spatial variability of crop biophysical variables. Besides bare soil plots represented in red, three major groups of plots can be seen in the image corresponding to low (blue), intermediate (mainly yellow), and high (green) chlorophyll levels, the mean values of which were determined as 28, 41, and 48 μg/cm^2, respectively. The corresponding standard deviation values are estimated to 4.58, 2.71, and 1.77, respectively. The mean value of 41 μg/cm^2 for the intermediate group is due to the presence of high chlorophyll areas within some plots. These are in agreement with the expected spatial variability to result from nitrogen fertilization differences: high nitrogen levels, generating high chlorophyll concentrations, should induce a spatial homogeneity of crop biophysical properties. This is corroborated by the decrease of variability when chlorophyll content increases from 28 to 48 μg/cm^2. The spatial heterogeneity of CASI-estimated chlorophyll and its comparison with ground truth data are thoroughly analyzed and discussed by Haboudane et al. (2001) and Tremblay et al. (2001).

4. Conclusion

In this study, leaf and canopy models (PROSPECT and SAILH) were employed to simulate chlorophyll and LAI effects on crop canopy reflectance. Then, a methodology for predicting chlorophyll status from hyperspectral data, based on combining vegetation and chlorophyll indices through scaling up, has been developed and successfully tested with airborne CASI hyperspectral images over a corn crop experimental site.

The methodology was used to investigate and take into account the effects of nonphotosynthetic materials and LAI on the retrieval of leaf chlorophyll at the canopy level. To address these issues, we developed a transformed variant of the chlorophyll index MCARI, called TCARI, which is more sensitive to low chlorophyll values and more resistant to vegetation nonphotosynthetic materials. Then, a vegetation index that minimizes soil effects on the canopy reflectance (OSAVI) has been integrated with TCARI to remove LAI influence on chlorophyll predictions from remotely sensed data. The study has shown that the chlorophyll content is correlated with the slope of TCARI versus OSAVI, and has demonstrated that the ratio TCARI/OSAVI is insensitive to LAI variations, for LAI values ranging from 0.5 to 8. Consequently, a predictive function, independent of LAI, can be developed through modeling to map crop chlorophyll status using airborne remote sensing images. Resulting chlorophyll content estimations showed a very good agreement with laboratory chlorophyll measurements, with a high correlation coefficient (r=.9) and RMSE of 4.35 $\mu g/cm^2$.

The method proposed in this paper holds a strong potential for "operational" use in the context of precision agriculture. It allows an accurate estimation of crop photosynthetic pigments without a priori knowledge of the canopy architecture. However, the actual robustness of this methodology and its use needs to be verified in early growth conditions when LAI is low, as this is when such potential information is most critical for operational use. This method should be valuable for other crops as well, and further work should focus on developing a single and simple index that will have the same predictive capabilities as the ratio TCARI/OSAVI. Particularly, it should analyze the right set of spectral bands, the combination of which will enhance sensitivity to chlorophyll content variations and reduce responsivity to background and canopy structure effects. Moreover, a careful analysis should be carried out to investigate the effects of band characteristics: centre location and bandwidth.

Acknowledgments

The authors gratefully acknowledge the financial support provided for this research by GEOIDE (GEOmatics Informed Decisions) and the Canadian Space Agency. We thank Lawrence Gray and Phil Brasher and Heidi Beck of Aviation International for making CASI airborne field campaigns work efficiently. Efforts by Elizabeth Pattey of Agriculture and Agri-Food Canada (Ottawa) for the coordination of the CASI missions with field data collection are much appreciated. We gratefully acknowledge Craig S. T. Daughtry of the USDA ARS Hydrology and Remote Sensing Laboratory for his exchanges regarding CARI and MCARI indices. We also thank Carl Bélec, Marcel Tétreault, and the staff of the L'Acadie Experimental Farm for their contribution to the experimentation. Finally, we are indebted to Alain Viau of Laval University whose contributions to the overall coordination and management of the GEOIDE project made this research possible.

References

Adams, M. L., Norvell, W. A., Philpot, W. D., & Peverly, J. H. (2000a). Spectral detection of micronutrient deficiency in 'Bragg' soybean. *Agronomy Journal*, *92*, 261–268.

Adams, M. L., Norvell, W. A., Philpot, W. D., & Peverly, J. H. (2000b). Toward the discrimination of manganese, zinc, copper, and iron in deficiency 'Bragg' soybean using spectral detection methods. *Agronomy Journal*, *92*, 268–274.

Adams, M. L., Philpot, W. D., & Norvell, W. A. (1999). Yellowness index: an application of spectral second derivatives to estimate chlorosis of leaves in stressed vegetation. *International Journal of Remote Sensing*, *20*, 3663–3675.

AERONET (2000). *Ground-based remote sensing aerosol network.* Available at: http://aeronet.gsfc.nasa.gov:8080/.

Baret, F., Guyot, G., & Major, D. (1989). TSAVI: a vegetation index which minimizes soil brightness effects on LAI and APAR estimation. *Proceedings of 12th Canadian Symposium on Remote Sensing and IGARSS'89, Vancouver, Canada, 10–14 July 1989* (pp. 1355–1358).

Blackburn, G. A. (1998a). Spectral indices for estimating photosynthetic pigment concentrations: a test using senescent tree leaves. *International Journal of Remote Sensing*, *19*, 657–675.

Blackburn, G. A. (1998b). Quantifying chlorophylls and carotenoids from leaf to canopy scale: an evaluation of some hyperspectral approaches. *Remote Sensing of Environment*, *66*, 273–285.

Blackburn, G. A. (1999). Relationships between spectral reflectance and pigment concentrations in stacks of deciduous broadleaves. *Remote Sensing of Environment*, *70*, 224–237.

Blackmer, T. M., Schepers, J. S., & Varvel, G. E. (1994). Light reflectance compared with other nitrogen stress measurements in corn leaves. *Agronomy Journal*, *86*, 934–938.

Blackmer, T. M., Schepers, J. S., Varvel, G. E., & Walter-Shea, E. A. (1996). Nitrogen deficiency detection using reflected shortwave radiation from irrigated corn canopies. *Agronomy Journal*, *88*, 1–5.

Boissard, P., Pointel, J.-G., & Huet, P. (1993). Reflectance, green leaf area index and ear hydric status of wheat from anthesis until maturity. *International Journal of Remote Sensing*, *14*, 2713–2729.

Chappelle, E. W., Kim, M. S., & McMurtrey III, J. E. (1992). Ratio analysis of reflectance spectra (RARS): an algorithm for the remote estimation of the concentrations of chlorophyll *A*, chlorophyll *B*, and the carotenoids in soybean leaves. *Remote Sensing of Environment*, *39*, 239–247.

Clevers, J. G. P. W. (1997). A simplified approach for yield prediction of sugar beet based on remote sensing data. *Remote Sensing of Environment*, *61*, 221–228.

Clevers, J. G. P. W., Büker, C., van Leeuwen, H. J. C., & Bouman, B. A. M. (1994). A framework for monitoring crop growth by combining directional and spectral remote sensing information. *Remote Sensing of Environment*, *50*, 161–170.

Datt, B. (1999). A new reflectance index for remote sensing of chlorophyll content in higher plants: tests using eucalyptus leaves. *Journal of Plant Physiology*, *154*, 30–36.

Daughtry, C. S. T., Walthall, C. L., Kim, M. S., Brown de Colstoun, E., & McMurtrey III, J. E. (2000). Estimating corn leaf chlorophyll concentration from leaf and canopy reflectance. *Remote Sensing of Environment*, *74*, 229–239.

Demarez, V., & Gastellu-Etchegorry, J. P. (2000). A modeling approach for studying forest chlorophyll content. *Remote Sensing of Environment*, *1*, 226–238.

Erol, H., & Akdeniz, F. (1996). A multispectral classification algorithm for classifying parcels in an agricultural region. *International Journal of Remote Sensing*, *17*, 3357–3371.

Gitelson, A. A., Merzyak, M. N., & Lichtenthaler, H. K. (1996). Detection of red edge position and chlorophyll content by reflectance measurements near 700 nm. *Journal of Plant Physiology*, *148*, 501–508.

Goel, N. S. (1988). Models of vegetation canopy reflectance and their use in estimation of biophysical parameters from reflectance data. *Remote Sensing Reviews*, *4*, 1–212.

Goel, N. S. (1989). Inversion of canopy reflectance models for estimation of biophysical parameters from reflectance data. In: G. Asrar (Ed.), *Theory and applications of optical remote sensing* (pp. 205–251). New York: Wiley.

Grignetti, A., Salvatori, R., Cascchia, R., & Manes, F. (1997). Mediterranean vegetation analysis by multitemporal satellite data. *International Journal of Remote Sensing*, *18*, 1307–1318.

Haboudane, D., Miller, J. R., Tremblay, N., Zarco-Tejada, P. J., Dextraze, L., & Viau, A. (2001). Heterogeneity of CASI-estimated leaf chlorophyll in corn: assessment and comparison with ground truth from L'Acadie GEOIDE experimental site. *Proceedings of the 23rd Canadian Symposium on Remote Sensing and 10th Congress of the Quebec Remote Sensing Association, Université Laval University Sainte-Foy, Quebec, Canada, 21–24 August 2001*.

Hapke, B. (1993). *Theory of reflectance and emittance spectroscopy* (p. 469). Cambridge, UK: Cambridge University Press.

Huete, A. R. (1988). A soil-adjusted vegetation index (SAVI). *Remote Sensing of Environment*, *25*, 295–309.

Jacquemoud, S., Bacour, C., Poilve, H., & Frangi, J.-P. (2000). Comparison of four radiative transfer models to simulate plant canopies reflectance: direct and inverse mode. *Remote Sensing of Environment*, *74*, 417–481.

Jacquemoud, S., & Baret, F. (1990). Prospect: a model for leaf optical properties spectra. *Remote Sensing of Environment*, *34*, 75–91.

Jacquemoud, S., Ustin, S. L., Verdebout, J., Schmuck, G., Andreoli, G., & Hosgood, B. (1996). Estimating leaf biochemistry using the PROSPECT leaf optical properties model. *Remote Sensing of Environment*, *56*, 194–202.

Kim, M. S., Daughtry, C. S. T., Chappelle, E. W., McMurtrey III, J. E., & Walthall, C. L. (1994). The use of high spectral resolution bands for estimating absorbed photosynthetically active radiation (Apar). *Proceedings of the 6th Symposium on Physical Measurements and Signatures in Remote Sensing, January 17–21, 1994, Val D'Isere, France* (pp. 299–306).

Kuusk, A. (1985). The hot spot effect on a uniform vegetative cover. *Soviet Journal of Remote Sensing*, *3*, 645–658.

Malthus, T. J., & Madeira, A. C. (1993). High resolution spectroradiometry: spectral reflectance of field bean leaves infected by *Botrytis fabae*. *Remote Sensing of Environment*, *45*, 107–116.

Moran, M. S., Inoue, Y., & Barnes, E. M. (1997). Opportunities and limitations for image-based remote sensing in precision crop management. *Remote Sensing of Environment*, *61*, 319–346.

Moran, M. S., Maas, S. J., & Pinter Jr., P. J. (1995). Combining remote sensing and modeling for estimating surface evaporation and biomass production. *Remote Sensing of Environment*, *12*, 335–353.

O'Neill, N. T., Zagolski, F., Bergeron, M., Royer, A., Miller, R. J., & Freemantle, J. (1997). Atmospheric correction validation of CASI images acquired over the BOREAS southern study area. *Canadian Journal of Remote Sensing*, *23*, 143–162.

Pax-Lenney, M., & Woodcock, C. E. (1997). The effect of spatial resolution on the ability to monitor the status of agricultural lands. *Remote Sensing of Environment*, *61*, 210–220.

Porra, R. J., Thompson, W. A., & Kriedemann, P. E. (1989). Determination of accurate extinction coefficients and simultaneous equations for assaying chlorophylls *a* and *b* extracted with four different solvents: verification of the concentration of chlorophyll standards by atomic absorption spectroscopy. *Biochimica et Biophysica Acta*, *975*, 384.

Potdar, M. B. (1993). Sorghum yield modelling based on the crop growth parameters determined from visible and near-IR channel NOAA AVHRR data. *International Journal of Remote Sensing*, *14*, 895–905.

Rasmussen, M. S. (1992). Assessment of millet yields and production in northern Burkina Faso using integrated NDVI from the AVHRR. *International Journal of Remote Sensing*, *13*, 3431–3442.

Rondeaux, G., Steven, M., & Baret, F. (1996). Optimization of soil-adjusted vegetation indices. *Remote Sensing of Environment*, *55*, 95–107.

Tremblay, N., Miller, J., Haboudane, D., Bélec, C., & Dextraze, L. (2001). Effect of nitrogen fertility status on uniformity of growth, yield and pigment concentration of corn canopies. *Third International Conference on Geospatial Information in Agriculture and Forestry, Denver, CO, 5–7 November 2001*.

Tucker, C. J., Holben, B. N., Elgin Jr., J. H., & McMurtrey, J. E. (1980). Relationship of spectral data to grain yield variations. *Photogrammetric Engineering and Remote Sensing*, *46*, 657–666.

Verhoef, W. (1984). Light scattering by leaf layers with application to canopy reflectance modeling: the SAIL model. *Remote Sensing of Environment*, *16*, 125–141.

Verhoef, W. (1998). *Theory of radiative transfer models applied in optical remote sensing of vegetation canopies*. Wageningen: Grafish Service Centrum Van Gils.

Walburg, G., Bauer, M. E., Daughtry, C. S. T., & Housley, T. L. (1982). Effects of nitrogen nutrition on the growth, yield and reflectance characteristics of corn canopies. *Agronomy Journal*, *74*, 677–683.

Wood, C. W., Reeves, D. W., & Himelrick, D. G. (1993). Relationship between chlorophyll meter readings and leaf chlorophyll concentration, N status, and crop yield: a review. *Proceedings of the Agronomy Society of New Zealand*, *23*, 1–9.

Zarco-Tejada, P. J. (2000). *Hyperspectral remote sensing of closed forest canopies: estimation of chlorophyll fluorescence and pigment content.* PhD thesis, Graduate programme in Earth and Space Science, York University, Toronto, Ontario, Canada, 210 pp.

Zarco-Tejada, P. J., Miller, J. R., Mohammed, G. H., Noland, T. L., & Sampson, P. H. (2000). Chlorophyll fluorescence effects on vegetation apparent reflectance: II. Laboratory and airborne canopy-level measurements with hyperspectral data. *Remote Sensing of Environment*, *74*, 596–608.

Zarco-Tejada, P. J., Miller, J. R., Noland, T. L., Mohammed, G. H., & Sampson, P. H. (2001). Scaling-up and model inversion methods with narrow-band optical indices for chlorophyll content estimation in closed forest canopies with hyperspectral data. *IEEE Transactions on Geoscience and Remote Sensing*, *39*, 1491–1507.